INL/CON-14-33350
PREPRINT

The IAEA Coordinated Research Program on HTGR Uncertainty Analysis: Phase I Status and Initial Results

Proceedings of HTR 2014

Frederik Reitsma, Gerhard Strydom,
Friederike Bostelmann, Kostadin Ivanov

October 2014

The INL is a
U.S. Department of Energy
National Laboratory
operated by
Battelle Energy Alliance

Proceedings of HTR 2014
Weihai, China, October 27 – 31, 2014
Paper HTR2014-51106

The IAEA Coordinated Research Program on HTGR Uncertainty Analysis: Phase I Status and Initial Results

Frederik Reitsma, Gerhard Strydom [1], Friederike Bostelmann [1], Kostadin Ivanov [2]

Division of Nuclear Power, International Atomic Energy Agency (IAEA)
Vienna International Centre, PO Box 100, A-1400 Vienna, Austria
phone: +43-(1)2600-22565, F.Reitsma@iaea.org

[1] Nuclear Science and Engineering Division
Idaho National Laboratory (INL)
Idaho Falls, ID83415, U.S.A.

[2] Nuclear Engineering, The Pennsylvania State University (PSU)
230 Reber Building, University Park, PA 16802, U.S.A.

Abstract – *The quantification of uncertainties in design and safety analysis of reactors is today not only broadly accepted, but in many cases became the preferred way to replace traditional conservative analysis for safety and licensing analysis. The use of a more fundamental methodology is also consistent with the reliable high fidelity physics models and robust, efficient, and accurate codes available today. To facilitate uncertainty analysis applications a comprehensive approach and methodology must be developed and applied. This is in contrast to the historical approach where sensitivity analysis were performed and uncertainties then determined by a simplified statistical combination of a few important input parameters. New methodologies are for example under development in the OECD/NEA Light Water Reactor (LWR) Uncertainty Analysis in Best-Estimate Modelling (UAM) benchmark activity. High Temperature Gas-cooled Reactors (HTGR) has its own peculiarities, coated particle design, large graphite quantities, different materials and high temperatures that also require other simulation requirements. The IAEA has therefore launched a Coordinated Research Project (CRP) on the HTGR Uncertainty Analysis in Modelling in 2013 to study uncertainty propagation specifically in the HTGR analysis chain. Two benchmark problems are defined, with the prismatic design represented by the General Atomics (GA) MHTGR-350 and a 250 MW modular pebble bed design similar to the HTR-PM (INET, China). Work has started on the first phase and the current status is reported in the paper.*

I. INTRODUCTION

The continued development of High Temperature Gas Cooled Reactors (HTGRs) requires verification of HTGR design and safety features with reliable high fidelity physics models and robust, efficient, and accurate codes. One way to address the uncertainties in the HTGR analysis tools are to assess the sensitivity of critical parameters (such as the calculated maximum fuel temperature during loss of coolant accidents) to a few important input uncertainties. The input parameters were identified by engineering judgement in the past but are today typically based on a Phenomena Identification Ranking Table (PIRT) process. The input parameters can also be derived from sensitivity studies and are then varied in the analysis to find a spread in the parameter of importance [1]. However, there is often no easy way to compensate for these uncertainties. In engineering system design, a common approach

for addressing performance uncertainties is to add compensating margins to the system, but with passive properties credited it is not so clear how to apply it in the case of modular HTGR heat removal path [2]. Other more sophisticated uncertainty modelling approaches, including Monte Carlo analysis, have also been proposed and applied [3].

Ideally one wishes to apply a more fundamental approach to determine the predictive capability and accuracies of coupled neutronics/thermal-hydraulics and depletion simulations used for reactor design and safety assessment [4]. Today there is a broader acceptance of the use of uncertainty analysis even in safety studies and it has been accepted by regulators in some cases to replace the traditional conservative analysis. Therefore some safety analysis calculations may use a mixture of these approaches for different parameters depending upon the particular requirements of the analysis problem involved. Sensitivity analysis can for example be used to provide information as part of an uncertainty analysis to determine best estimate plus uncertainty results to the required confidence level [5].

In order to address uncertainty propagation in analysis and methods in the HTGR community the IAEA initiated a Coordinated Research Project (CRP) on the HTGR Uncertainty Analysis in Modelling (UAM) [6] that officially started in 2013. Although this project focuses specifically on the peculiarities of HTGR designs and its simulation requirements, many lessons can be learned from the LWR community and the significant progress already made towards a consistent methodology uncertainty analysis.

In the case of LWRs the NRC has already in 1988 amended 10 CFR 50.46 to allow best-estimate (plus uncertainties) calculations of emergency core cooling system performance. The Nuclear Energy Agency (NEA) of the Organization for Economic Co-operation and Development (OECD) also established an Expert Group on "Uncertainty Analysis in Modelling" which finally led to the definition of the "Benchmark for Uncertainty Analysis in Modelling (UAM) for Design, Operation and Safety Analysis of LWRs" [7]. The CRP on HTGR UAM will follow as far as possible the on-going OECD Light Water Reactor UAM benchmark activity.

In order to benefit from recent advances in modelling and simulation and the availability of new covariance data (nuclear data uncertainties) extensive sensitivity and uncertainty studies are needed for quantification of the impact of different sources of uncertainties on the design and safety parameters of HTGRs. Only a parallel effort in advanced simulation and in nuclear data improvement will be able to provide designers with more robust and well validated calculation tools to meet design target accuracies.

Uncertainty and sensitivity studies are an essential component of any significant effort in data and simulation improvement. These studies can also be used in a convincing and effective manner to perform design optimization and to assess safety features and design margins, but only if the uncertainty information is of the highest quality, reliability and science-based.

II. CRP ON HTGR UAM OVERVIEW

The proposed technical approach is to establish and utilize a benchmark for uncertainty analysis in best-estimate coupled HTGR modelling and analysis, using as a basis a series of well-defined problems with complete sets of input specifications and as far as possible reference experimental data.

The principal idea is to subdivide the coupled system calculation into several steps, each of which can contribute to the total uncertainty and to identify input, output, and assumptions for each step. The resulting uncertainty in each step will be calculated by taking into account all sources of uncertainties including propagating the related uncertainties from previous steps. The four phases are as follows:

- Phase I (Local Standalone Modelling)
- Phase II (Global Standalone Modelling)
- Phase III (Design Calculations)
- Phase IV (Safety Calculations)

Two main HTGR types have been selected based on previous benchmark experiences and available data: a 250MWth pebble bed design based on the HTR-Module [8], and a 350MWth prismatic design based on the Modular High Temperature Gas Reactor (MHTGR) [9]. A detailed description of the two reactor designs, detailed background information and an explanation of the methodology to be followed can be found in [10].

The benchmark specification for Phase I requires the modelling of local effects. It is divided into the following exercises.

II.A. Phase I

Exercise I-1: "Local Neutronics"

This exercise is focused on the derivation of the multi-group microscopic cross-section libraries. Its objective is to address the uncertainties due to the basic nuclear data as well as the impact of

processing the nuclear and covariance data, selection of multi-group structure, and double heterogeneity or self-shielding treatment. The intention is to propagate the uncertainties in evaluated Nuclear Data Libraries - NDL - (microscopic point-wise cross sections) into multi-group microscopic cross-sections. Exercises I-1a and I-1b are defined to capture the local neutronics effects.

Exercise I-1a/b – Cell Physics: Derivation of the multi-group microscopic cross-section libraries.

The single pebble unit cell, shown in Fig. 1~~Fig. 1~~, represents a pebble with a given burnup and with number-densities provided for the main actinides and fission products. The reflective boundary condition implies that it is surrounded by the same fuel type. The unit cell for the MHTGR prismatic design is likewise defined, as shown in Fig. 2~~Fig. 2~~. Both specifications include number density and geometry data for the (Xenon-free) Cold Zero Power (CZP) and Hot Full Power (HFP) conditions to study the effect of an increase in temperature. The homogeneous (TRISO and compact matrix material volume-averaged) version of the specification is designated as Ex. I-1a, while Ex. I-1b requires the explicit modelling of the TRISO fuel kernels.

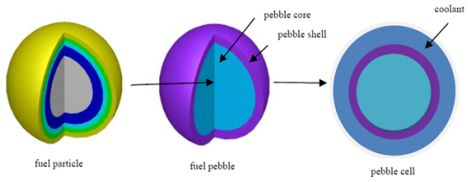

Fig. 1: Single pebble unit cell.

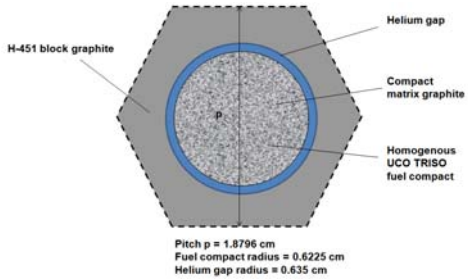

Fig. 2: Single MHTGR fuel compact unit cell.

Exercise I-2 – Lattice Physics: Derivation of the few-group macroscopic cross-section libraries

In this case the correct environment of the pebble fuel needs to be taken into account in a "lattice physics" model. The target is to obtain few group parameters, variance / co-variance matrix for all homogenized cross-sections including diffusion coefficients, Assembly Discontinuity Factors (ADFs), where applicable, and kinetic parameters.

One important issue in this exercise is the definition of a lattice. For the pebble reactor design the following considerations will be taken into account:

- one dimensional (1D) core calculation
- single pebble with different leakage conditions
- multiple pebbles (mixture of different compositions / burnup)

The 1D cut (slab or cylindrical) through the core is typically modelled of infinite height (random packing) with reflectors modelled in a mini-core as shown in Fig. 3~~Fig. 3~~. The two alternative models are much simpler but rely on the definition of the correct mixtures and boundary conditions to try and represent the neutron spectrum in the core correctly. These are shown in Fig. 4~~Fig. 4~~.

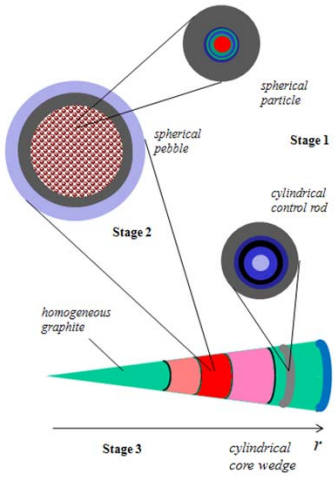

Fig. 3: Mini-core one-dimensional lattice cell.

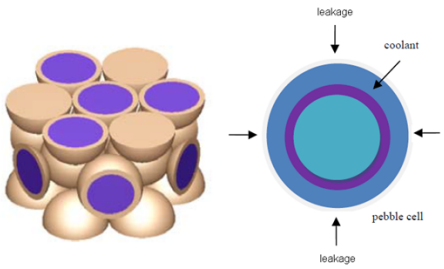

Fig. 4: Alternative lattice cell definitions.

For the prismatic lattice physics calculation, the geometry and number density data for a single MHTGR-350 hexagonal fuel block (shown in Fig. 5~~Fig. 5~~) is provided. A second variation of this problem adds the spectral effects of neighbouring blocks, as shown in the "supercell" Fig. 6~~Fig. 6~~.

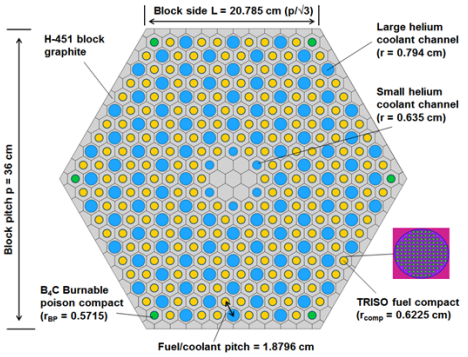

Fig. 5: MHTGR-350 lattice cell for Ex. I-2a (fresh single block).

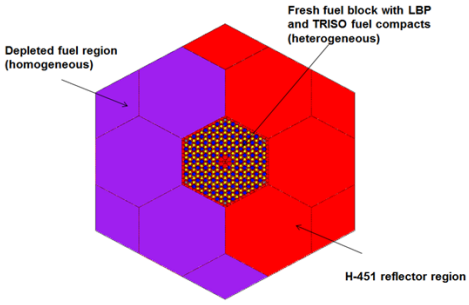

Fig. 6: Graphical Representation of Ex.I-2c Super-Cell.

Initial results will be presented in Section III (SCALE/KENO-VI and Serpent) and Section IV (SCALE/TSUNAMI) of this paper for Ex. I-1a and I-1b of the prismatic reactor design. The reference results for the prismatic Ex. I-3a and I-3b (stand-alone steady-state and transient thermal hydraulics cell calculations) were reported earlier in 2014 [11] .

II.B. Phases II-IV

The following cases are currently included in the benchmark specification for Phases II-IV (more detail can be found in [10]):

Phase II: Global Standalone Modelling

- Exercise II-1a: Core physics: Criticality stand-alone neutronics.
- Exercise II-1b: Core physics: Stand-alone kinetics without feedback.
- Exercise II-2a/b: Stand-alone thermal-hydraulics focused on core thermal-hydraulic modelling (normal operation / Depressurized Loss of Forced Cooling transient).

Phase III: Design Calculations

- Exercise III-1: Coupled neutronics and thermal hydraulic steady-state.
- Exercise III-2: Coupled depletion and neutronics.

Phase IV: Safety Calculations

- Exercise IV-1: Coupled core transient.
- Exercise IV-2: Coupled system transient.

III. EX. I-1A AND I-1B REFERENCE RESULTS

A limited literature survey found several HTGR lattice calculation comparisons between heterogeneous and homogeneous fuel, double heterogeneity treatments (including random vs. regular particle distributions), Monte Carlo and deterministic transport codes, and continuous-energy and multi-group criticality calculations. Comparative data sets are available for both pebble bed ([12]-[14]) and prismatic high temperature reactors ([15]~~[16]~~-[20]).

In this paper, simulations have been performed with the Monte Carlo codes Serpent [21] and SCALE/KENO-VI [22] on a fresh fuel compact unit cell of the MHTRG-350 HTGR, as described in Section II. In addition to a comparison of the codes and the fuel region treatment, KENO-VI calculations for continuous-energy and multi-group libraries have been performed, and the results obtained are compared with a sub-set of the existent body of literature.

In the absence of experimental data, the results of the Serpent calculations are used as the reference for comparisons with the KENO-VI calculations, due to Serpent's capability to produce a continuous energy solution with a random particle distribution in the fuel cell.

III.A Computer Codes and Models

The Serpent Monte Carlo Code is a three-dimensional continuous-energy neutron transport code, and has been developed at the VTT Technical Research Centre of Finland since 2004. It is capable of simulating various fuel assembly geometries, perform burn-up calculations and can also be utilized for the simulation of smaller reactor cores [21][~~21~~]. In order to provide a better parallelization of the program and the possibility of performing three-dimensional burn-up calculations, the Serpent code has been rewritten, and the latest version (Serpent 2) is scheduled to be released by the end of 2014. A beta version is currently available for licensed users.

For the calculations reported in this paper, the latest beta version of Serpent 2 (version 2.1.21) was used. In order to perform additional calculations using the ENDF-B-VII.1 cross section data library, the source code of this version was slightly modified by the code developer, J. Leppänen. This modification will be included in the next release of Serpent 2 [23][~~23~~]. Since Serpent 2 provides the capability of performing parallel calculations using a combination of MPI and OpenMP parallelization, the calculations were performed on a High Performance Computing system, typically utilizing 3 nodes (a total of 96 processors).

The KENO-VI module of the SCALE 6.1 code package was developed at Oak Ridge National Laboratory (ORNL). It is a high-fidelity three-dimensional Monte Carlo criticality code, and ENDF-B-VII.0 continuous-energy or 238 multi-group cross section data libraries can be applied [22][~~22~~]. (The ENDF-B-VII.1 library is not yet available for use in SCALE).

In addition to the current SCALE 6.1.2 release, results generated by a beta release of SCALE 6.2 (beta version 3) has also been included in this study. This version includes a new 252-group library that is optimized for LWR applications. The relative performance of this library for this HTGR application is also reported here. It should be noted that ORNL also developed a dedicated HTGR 81-group library in 2012 that produced very similar results compared to the 238-group library, without the latter's run-time penalty [24]. Unfortunately this library is not implemented in the current versions of SCALE. All SCALE calculations were performed on a single processor, and although version 6.2b3 can be compiled to perform parallel KENO-VI and SAMPLER (see Section IV) computations, this option was not pursued yet.

Ex. I-1a Serpent model

The homogeneous unit cell is modeled as a two-dimensional cell with reflective boundary conditions in all directions. Temperatures for the CZP and HFP states were considered via Doppler broadening. In terms of carbon, the natural composition of carbon was applied in all materials. Furthermore carbon was always considered as graphite, i.e. the thermal scattering data for graphite was applied. Additionally, Doppler-broadening rejection correction for U-238 has been applied [25]. All simulations were performed using the ENDF-B-VII.0 and ENDF-B-VII.1 continuous-energy cross section data libraries.

For each Serpent Monte Carlo simulation, 1,000 active neutron cycles with 25,000 neutrons per cycle were calculated. The first 100 cycles were skipped and not considered in the evaluation of the multiplication factor. Each of the Serpent runs was typically completed within 23 minutes, using a combination of 12 MPI and 8 OMP jobs.

Ex. I-1a KENO-VI model

The KENO-VI model is equivalent to the Serpent model, but extended in a third dimension, for which the compact height (4.928 cm) was used. Simulations of both CZP and HFP core states using ENDF-B-VII.0 continuous-energy (CE) and multi-group (MG) cross section libraries were performed. In case of the MG cross sections, the lattice cell treatment and the 238-group library was applied. An additional calculation was performed using the 252-group library of SCALE 6.2b3. KENO-VI simulations were performed for 500 active neutron cycles and 50,000 neutrons per cycle, with 50 cycles initially skipped. Each of the KENO-VI CE runs typically took 230 minutes to complete on a single processor, and the equivalent MG runs 130 minutes.

Ex. I-1b Serpent model

Exercise I-1b requires explicit modeling of the TRISO fuel particles. In order to realize an explicit model, the two-dimensional model was extended to a three-dimensional model with the height of one fuel compact. The reflective boundary condition in all directions was retained.

Serpent provides the option to disperse the particles randomly in a given volume. After entering the particle specifications, the compact dimensions and the packing fraction, Serpent created a file with the positions of 6647 randomly distributed particles in the compact (Fig. 7).

Formatted: Font color: Text 1

Formatted: Font color: Text 1

Formatted: Font color: Text 1

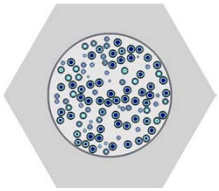

Fig. 7: Cross-sectional view of the Serpent model for Ex. I-1b with randomly distributed TRISO particles.

Additionally, a second model with particles in a regular grid was created. To distribute the particles as uniformly as possible, a layer of 133 particles in a square lattice with a pitch of 0.091 cm was created (Fig. 8). All particles are contained within the cylindrical fuel compact region, i.e. no particles were cut by the outer boundary. A stack of 50 particle layers with a height of 0.09856 cm each made up a fuel compact. Altogether 6650 particles are inserted in the compact in this manner, and the average packing fraction in the compact is therefore slightly increased to 35.02 %. Due to larger distances between the particles and the cylinder, the local packing fraction in one lattice cell increased to about 38.7 %. With the same settings as in Ex. I-1a, these simulations took about 25 minutes.

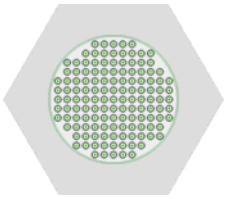

Fig. 8: Cross-sectional view of the Serpent model for Ex. I-1b with uniformly distributed TRISO particles.

Ex. I-1b KENO-VI model

The KENO-VI model for Exercise I-1b corresponds with the Serpent model for regularly distributed TRISO particles in the compact, since the standard geometry options in KENO-VI do not include a random particle distribution. The reflective boundary condition was retained, and for the MG calculations, the DOUBLEHET cell data was specified to consider the double heterogeneous structure of the TRISO particles in the fuel compact [26]. Using the same settings as in Ex. I-1a, the CE simulation took about 60 hours and the MG simulation about 140 minutes.

III.B. Ex. I-1a Reference Results

The results of Exercise I-1a are summarized in Table 1. Although the ENDF-B-VII.1 data library is the latest release, the Serpent result using the ENDF-B-VII.0 library is taken as the reference result for this comparison. This allows a meaningful comparison with the KENO-VI results, which are currently limited to the ENDF-B-VII.0 data library.

It is observed that the use of the ENDF-B-VII.1 data lead to infinite multiplication factors (k_∞) approximately 100 pcm lower than the ENDF-B-VII.0 values. Goto [15] ascribed these differences to an underestimation of the carbon neutron capture cross section at thermal energies in the ENDF-B-VII.0 library. The correction of this cross section in ENDF-B-VII.1 resulted in increased neutron capture and thus a reduction in the multiplication factor.

The HFP k_∞ are furthermore up to 7500 pcm lower than the CZP k_∞ values. These differences are a primarily the result of ^{238}U Doppler resonance broadening.

The KENO-VI CE calculation shows good agreement with the Serpent value, with an overestimation of k_∞ by 51 pcm for the CZP state. The MG calculation of SCALE 6.1.2, however, underestimates the reference Serpent value by 410 pcm, and the SCALE 6.2b3 MG calculation by 445 pcm. These results do not have overlapping error bars by a narrow margin. The SCALE 6.2b3 MG calculation using 252 groups agrees with the SCALE 6.1.2 238 group calculation within one standard deviation, i.e. a somewhat better match than the 238 group comparison.

In contrast to the well-matched CZP state, the KENO-VI CE calculation of the HFP state overestimates the Serpent reference result by 360 pcm. As in the CZP state, the MG calculations show smaller multiplication factors. The simulations of both SCALE versions using 238 groups are within the standard deviation of the reference calculations. The 252-group calculation using SCALE 6.2b3, however, overestimates the reference by 96 pcm. It should however be kept in mind that both of these libraries are optimized for LWR applications, and that version 6.2b3 might still be modified before the first production release of Scale 6.2 by the end of 2014.

III.C. Ex. I-1b Reference Results

The results of Ex. I-1b are summarized in Table 2. The Serpent model including the random particle distribution using ENDF-B-VII.0 cross sections is used as the reference.

Table 1: Multiplication factor for Exercise I-1a

Model	CZP		HFP	
	$k_\infty \pm \sigma$	$\Delta \pm \sigma$ [pcm]	$k_\infty \pm \sigma$	$\Delta \pm \sigma$ [pcm]
Serpent (ENDF-B-VII.0)	1.27827 ± 0.00013	(reference)	1.20302 ± 0.00014	(reference)
Serpent (ENDF-B-VII.1)	1.27710 ± 0.00013	- 117 ± 18	1.20210 ± 0.00014	- 92 ± 20
KENO-VI CE (6.1.2)	1.27878 ± 0.00015	51 ± 20	1.20662 ± 0.00018	360 ± 23
KENO-VI 238 MG (6.1.2)	1.27417 ± 0.00013	- 410 ± 18	1.20294 ± 0.00014	- 8 ± 20
KENO-VI 238 MG (6.2b3)	1.27382 ± 0.00020	- 445 ± 24	1.20299 ± 0.00023	- 3 ± 27
KENO-VI 252 MG (6.2b3)	1.27428 ± 0.00021	- 399 ± 25	1.20398 ± 0.00020	96 ± 24

Table 2: Multiplication factor for Exercise I-1b

Model	CZP		HFP	
	$k_\infty \pm \sigma$	$\Delta \pm \sigma$ [pcm]	$k_\infty \pm \sigma$	$\Delta \pm \sigma$ [pcm])
Serpent – random (ENDF-B-VII.0)	1.31625 ± 0.00012	*(reference)*	1.24383 ± 0.00013	*(reference)*
Serpent – random (ENDF-B-VII.1)	1.31469 ± 0.00012	- 156 ± 17	1.24271 ± 0.00013	- 112 ± 18
Serpent – regular lattice (ENDF-B-VII.0)	1.31906 ± 0.00012	281 ± 17	1.24672 ± 0.00013	289 ± 18
KENO-VI CE – regular lattice (6.1.2)	1.31675 ± 0.00016	50 ± 20	1.24805 ± 0.00017	422 ± 21
KENO-VI 238 MG/DOUBLEHET (6.1.2)	1.30842 ± 0.00013	- 783 ± 18	1.24037 ± 0.00013	- 346 ± 18
KENO-VI 238 MG/DOUBLEHET (6.2b3)	1.31021 ± 0.00019	- 604 ± 22	1.24192 ± 0.00021	- 191 ± 25
KENO-VI 252 MG/DOUBLEHET (6.2b3)	1.31053 ± 0.00019	- 572 ± 22	1.24309 ± 0.00019	- 74 ± 23

Table 3: Comparison between Exercise I-1a and I-1b

Model	CZP		HFP	
	$k_\infty \pm \sigma$	$\Delta \pm \sigma$ [pcm]	$k_\infty \pm \sigma$	$\Delta \pm \sigma$ [pcm]
Serpent – random (ENDF-B-VII.0): heterog.	1.31625 ± 0.00012	(reference)	1.24383 ± 0.00013	(reference)
Serpent (ENDF-B-VII.0): homogeneous	1.27827 ± 0.00013	- 3798 ± 18	1.20302 ± 0.00014	- 4081 ± 20
KENO-VI CE (6.1.2): homogeneous	1.27878 ± 0.00015	- 3747 ± 20	1.20662 ± 0.00018	- 3721 ± 23
KENO-VI 238 MG (6.1.2): homogeneous	1.27417 ± 0.00013	- 4208 ± 18	1.20294 ± 0.00014	- 4089 ± 20

The difference between the Serpent calculations using different ENDF-B data libraries is slightly larger compared to the trends observed for Ex. I-1a.

The Serpent calculation with the regular particle lattice reveals an overestimation of k_∞ about 280 pcm. Similar studies for prismatic HTGR lattice problems ([16],[19]), however, reported conflicting trends. The trend seems to be dependent on the modeling of the particle lattice. The particle lattice in this study considered the particle fraction only in the compact, but not in a lattice unit cell. If the local packing fraction is increased, a decrease of the multiplication factor is expected.

The CE KENO-VI calculation shows an overestimation of 50 pcm for the CZP state and an overestimation of 422 pcm for the HFP state. All MG calculations underestimate the respective reference result for the cold state by more than one standard deviation. This trend was also observed by Wang [27], Chiang [20] and Ilas [18] for the criticality calculations of the HTTR, a prismatic high temperature reactor with annular fuel compacts. The fuel compact simulations of Leppänen [16], however, revealed consistent simulations of the regular particle lattice with KENO-VI and Serpent, whereas we found differences of 231 pcm and 133 pcm for the cold and hot state, respectively. Since fuel and graphite temperatures might have a significant influence on this difference, and Leppänen did not include temperature-related information, a final conclusion cannot be reached at this point.

For both states the SCALE 6.2b3 calculations using 252 groups revealed a MG result that is the closest to the Serpent reference. The differences in k_∞ between the cold and the hot state due to resonance broadening are moreover more than 7200 pcm for the Serpent calculations, and about 6800 pcm for the KENO-VI calculations.

III.D. Comparison of Ex.I-1a and Ex.I-1b

The main differences between Ex. I-1a and 1b are presented in Table 3. The simulation of the homogeneous fuel region with Serpent underestimates the reference (explicit TRISO) result by about 3800 pcm in the cold state and more than 4000 pcm in the hot state. The respective KENO-VI result is only slightly closer to the reference with a deviation of more than 3700 pcm in both states. The deviations of the MG calculations from the reference result are somewhat larger still.

This result compares well with the results of Kim et al. [17], who found differences of 3840 pcm at 600 K and 4290 pcm at 1000 K for SCALE calculations of a single HTGR fuel pin. Wang [27], however, found a smaller difference of 416 pcm in a comparison of a homogeneous MG with a heterogeneous particle lattice CE calculation of the HTTR, which is quite in contrast to the trends observed here.

The normalized neutron flux in the Serpent unit cell is presented in Fig. 9. It can be seen that the homogeneous neutron flux per unit lethargy is lower than the heterogeneous flux values in a large part of the spectrum (the fluxes for the random and regular particle distribution are identical, and have not been compared here). This lower integrated neutron flux leads to the reduced multiplication factor. The increased multiplication factor with "fuel lumping" (explicit coated particles compared to a homogenised model) is of course expected due to the larger resonance escape probability. The spectrum shift of the thermal peak value from the cold to the hot state is also clearly visible.

It is also shown in Fig. 9 that the fast flux peak is higher than the thermal peak, i.e. different than the usual thermal HTGR spectrum. This is caused by the specific unit cell geometry: up to now, only a single fuel compact unit cell is calculated, not a block or a full reactor core. A comparison of unit cell and single block spectra already revealed a small shift in the relative amplitudes of the thermal and fast flux peaks, and this effect will increase as one move on to the super-cell (Fig. 6~~Fig. 6~~) and full core calculations. A similar unit cell spectrum has also been reported by Ellis in a very detailed 999 fine-group cell-weighted calculation [24]~~[24]~~.

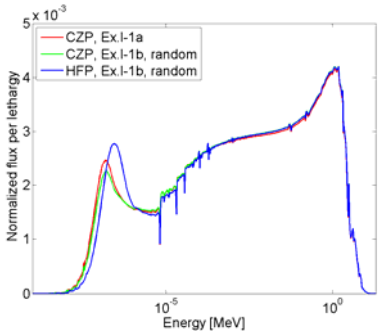

Fig. 9: Normalized neutron flux in the fuel compact unit cell.

A comparison of the capture cross section of ^{238}U is presented in Fig. 10 for three cases. The homogeneous calculation shows significant differences of more than 15% in the resonance region, while the CZP and HFP variances in the Ex.

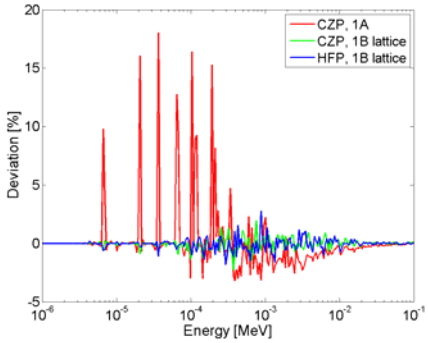

Fig. 10: Differences of the capture cross section of ^{238}U in the fuel compact unit cell for the Serpent calculation with random particle distribution.

I-1b lattice calculation are relatively small (< 3%).

Future work will involve the extension of these fuel compact unit cell models to fresh and depleted single fuel block models (Ex. I-2), as discussed in Section II. For an experimental validation of these exercises, the measured data of the VHTRC critical assembly [28] will be compared with the results obtained from MCNP, Serpent and SCALE simulations.

III.E. Influence of the Graphite Thermal Scattering Library

During our studies, the question of the treatment of carbon or graphite in the different materials arose. If the thermal scattering library for graphite is applied, a graphite crystal is assumed. In case of the fuel particle kernel material UCO and the silicon carbide layer, carbon does not form a graphite crystal. The treatment of carbon as graphite in these materials might therefore be wrong. Furthermore, the treatment of other materials containing only graphite is also questionable. Swanson and Harrison [29] suggested a mixture of bound-kernel graphite and free-gas sections to account for the fact that graphite is not a perfect crystal. Moreover, Hawari and Gillete [30] drew attention to the effects of graphite porosity on graphite neutron scattering.

Based on these suggestions, a sensitivity study consisting of three cases were performed with Serpent: (1) The carbon in all materials was treated as graphite, (2) Only the carbon in UCO and the silicon carbide layer was treated as elemental carbon, and (3) The carbon in all materials was treated as a mixture of 80% graphite and 20%. In all cases, the Ex. I-1b Serpent model was utilized.

Formatted: Font color: Text 1, English (U.K.)

Case (2) showed minor differences in k_∞ (in the order of one standard deviation) compared to case (1). The multiplication factor of case (3) revealed slightly higher deviations up to 83 ± 17 pcm from case (1). A specific bias can therefore not be observed from this limited dataset. A mixture of graphite and elemental carbon is moreover not a straightforward modification in the Serpent input. Furthermore, the treatment of carbon in the homogeneous fuel region of Ex. I-1a would also have to be modified if case (2) or (3) would be applied. On these grounds and because of the rather small differences between these cases, it is recommended that the CRP benchmark exercises should assume 100% graphite in all carbonaceous materials. This approach was followed in this paper.

IV. SCALE/TSUNAMI CROSS-SECTION UNCERTAINTY RESULTS FOR EX. I-1A

In addition to the reference "nominal case" results discussed in Section III for the prismatic design, the first uncertainty assessment results obtained for Ex. I-1a with SCALE/TSUNAMI (Tools for Sensitivity and Uncertainty Analysis Methodology Implementation) [22][~~22~~] are presented here. The TSUNAMI module utilizes data from the forward and adjoint transport solutions in an adjoint perturbation theory approach to generate sensitivity and uncertainty information. A cross-section library of covariance matrices for 401 nuclides in a 44-group energy structure are used to calculate the uncertainty on the integral parameters of interest (e.g. k_∞).

All the calculations presented here were performed with SCALE 6.1.2, but a new super-sequence SAMPLER [31] has also been developed for the beta releases of SCALE 6.2, and the result obtained with TSUNAMI will be compared in future publications. Since the current versions of TSUNAMI is not capable of generating data for systems that use the DOUBLEHET cell models (as would be required for Ex. I-1b and all subsequent HTGR exercises), the use of SAMPLER is the only method available in SCALE that can provide the correct implicit and explicit sensitivity coefficients. (The explicit sensitivity coefficients are determined from the flux perturbation that resulted from the perturbation of the multi-group cross sections, while the implicit sensitivity coefficients are associated with "self-shielded" perturbations; i.e. a perturbation in the cross section of a nuclide could change the self-shielded cross section of another nuclide, which in turn leads to additional flux perturbations).

Although it is well-known that the homogeneous treatment for HTGR designs are a basic modelling requirement, it was nevertheless decided to include Ex. I-1a as the first exercise to assess the differences that might result from this approach.

Using the same homogeneous unit cell definition as described in the previous section, KENO-IV obtained a forward best-estimate k_∞ = 1.27405 ± 0.00010, using 51x10^6 neutron histories. The adjoint KENO-IV calculation simulated 297x10^6 neutron histories to obtain an adjoint best-estimate k_∞ = 1.27270 ± 0.00130. (The relative difference ($k_{forward}$ - $k_{adjoint}$) of approximately 150 pcm falls within the TSUNAMI guidelines for the subsequent uncertainty analysis).

In the next uncertainty quantification step, the SCALE/SAMS module utilised the forward and adjoint flux data set to calculate a CZP k_∞ relative standard deviation of σ = 0.5409 ± 0.0002 % Δk/k due to the cross-section covariance data. The corresponding value for the HFP case is similar at σ = 0.5707 ± 0.0002 % Δk/k. The nuclide reaction covariance matrices responsible for the five largest contributions to the uncertainties in the CZP and HFP k-inf data are listed in Table 4. The largest k_∞ uncertainty contributor is the ^{238}U(n,γ) (capture) reaction, followed by the ^{235}U($\overline{\nu}$) and ^{235}U(n,γ) reactions. (Here, $\overline{\nu}$ is the average number of neutrons per fission reaction).

Table 4: The top 5 nuclide reaction covariance contributors to k_∞ uncertainty

Rank	Nuclide reaction	Uncertainty contribution due to this matrix (% Δk/k)	
		CZP	HFP
1	^{238}U(n,γ)	0.346	0.391
2	^{235}U($\overline{\nu}$)	0.269	0.267
3	^{235}U(n,γ)	0.247	0.245
4	U-238 elastic	0.124	0.130
5	C-graphite elastic	0.116	0.125

The contributions reported here for the homogenous prismatic HTGR unit cell is similar to the results obtained by for the equivalent cell exercises defined for Phase I of the OECD LWR UAM benchmark [7][~~7~~]. Mercatali [32][~~32~~] reports total uncertainties in k_∞ varying between 0.5%-0.6% for these thermal systems. The main differences between the HTGR and LWR/BWR Phase I results occur in the elastic scattering contributions of ^{238}U and graphite covariance matrices, as can be expected from a graphite moderator thermal system.

The sensitivity profiles are shown in Fig. 11~~Fig. 11~~ and Fig. 12~~Fig. 12~~ for the ^{238}U(n,γ), ^{235}U($\overline{\nu}$), ^{235}U(n,γ) and ^{238}U elastic scattering reactions. The contributions of the ^{238}U resonance region cross-sections can clearly be observed. The

Formatted: English (U.K.)

Formatted: English (U.K.)

Formatted: English (U.K.)

integral values indicated in the legends of the figures are the % change in k_∞ for a 1% increase in the respective nuclide cross-section, applied to all energy groups. For example, in Fig. 12~~Fig. 12~~ it is shown that a 1% increase in the $^{235}U(\overline{\nu})$ cross-section would lead to a change in k_∞ of 0.99%.

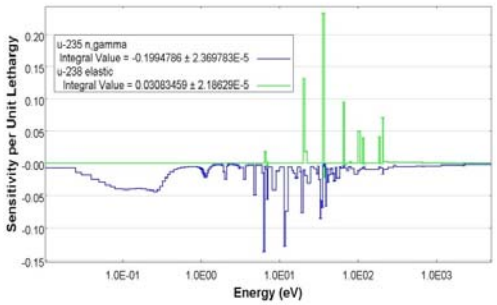

Fig. 11: k_∞ Sensitivity profiles for the $^{235}U(n,\gamma)$ and ^{235}U elastic scattering covariance matrices.

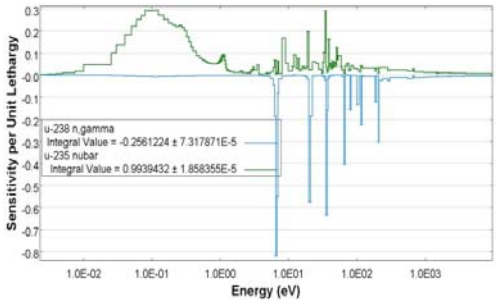

Fig. 12: k_∞ Sensitivity profiles for the $^{238}U(n,\gamma)$ and $^{235}U(\overline{\nu})$ covariance matrices.

V. SUMMARY

The Coordinated Research Programme on the uncertainties in HTGR coupled code modelling is a natural and logical continuation of previous international HTGR V&V activities.

This paper presented an overview of the CRP current status, as well as the first results for Exercises 1a and 1b of Phase 1 for the prismatic test cases. Reasonable agreement was found between the Serpent and SCALE/KENO Monte Carlo codes on the calculation of the reference results for the nominal Cold Zero and Hot Full Power cases, and the results of various sensitivity studies were also presented. The main contributors to the uncertainty in k_∞ were identified as the $^{238}U(n,\gamma)$ (capture) and $^{235}U(\overline{\nu})$ cross-section covariance matrices, and the total (one sigma) k_∞ uncertainty attributed to all cross-section covariances varied between 0.54% (CZP) and 0.57% (HFP).

The successful completion of the CRP on HTGR UAM is dependent on the availability of tools, software and data. The third beta release of SCALE 6.2 in June 2014 now allows the exploration of updated (KENO, TSUNAMI) and new (SAMPLER) tools. In the case of HTGR systems that require the treatment of double heterogeneity, the addition of the stochastic sequence SAMPLER is of specific interest to the HTGR community.

In 2014, scheduled CRP activities include the publication of updated Phase I and II specifications for the pebble bed and prismatic designs, as well as the second technical workshop that will be held in Vienna in December 2014.

REFERENCES

[1] G. Strydom, "TINTE uncertainty analysis of the maximum fuel temperature during a DLOFC event for the 400 MW Pebble Bed Modular Reactor", Proc. of ICAPP 2004, Pittsburgh, U.S.A., (2004).

[2] L.J. Lommers, B.E. Mays, F. Shahrokhi, "Passive heat removal impact on AREVA HTR design", *Nuclear Engineering and Design*, **271**, pp. 569-577 (2014)

[3] P. A. Jansen van Rensburg, M.G. Sage, "Uncertainty analysis for a depressurised loss of forced cooling event of the PBMR reactor", Proc. of ICONE14, Miami, U.S.A., (2006).

[4] C. Hao, F. Li, H. Zhang, "The challenges on uncertainty analysis for pebble bed HTGR", Proc. of PHYSOR 2012, Knoxville, U.S.A., (2012).

[5] LG-1045: "Guidance for licensing submissions involving computer software and evaluation models for safety calculations", National Nuclear Regulator, South Africa (2006).

[6] B.M. Tyobeka, et.al., "HTGR Reactor physics, thermal-hydraulics and depletion uncertainty analysis: a proposed IAEA coordinated research project", Proc. of M&C 2011, Rio de Janeiro, Brazil (2011).

[7] K. Ivanov, et al., "Benchmark for Uncertainty Analysis in Modelling (UAM) for Design, Operation and Safety Analysis of LWRs. Volume 1 – Specification and Supporting Data for Neutronics Cases (Phase I)", NEA/NSC /DOC(2013)7.

[8] H. Reutler, G.H. Lohnert, "Advantages of going modular in HTR's", *Nuclear Engineering and Design*, 78, pp. 129-136 (1984).

[9] A.S. Epiney, et al., "New multi-group transport neutronics (PHISICS) capabilities for RELAP5-3D and its application to phase I of the OECD/NEA MHTGR-350 MW benchmark", Proc. of HTR2012, Tokyo, Japan (2012).

[10] F. Reitsma, et. al., "The IAEA CRP on HTGR Reactor Physics, Thermal-hydraulics and Depletion Uncertainty Analysis", Proc. of HTR2012, Tokyo, Japan (2012).

[11] S.-J. Yoon, G. Strydom, "Comparison of homogeneous and heterogeneous CFD fuel models for phase I of the IAEA CRP on HTGR uncertainties benchmark", Proc. of ICAPP 2014, Charlotte, U.S.A., (2014).

[12] M.-J. Wang, et al., "Effects of geometry homogenization on the HTR-10 criticality calculations", *Nuclear Engineering and Design*, 271, pp. 356-360 (2014).

[13] M.-J. Wang, et al., "Criticality calculations of the HTR-10 pebble-bed reactor with SCALE6/CSAS6 and MCNP5", *Annals of Nuclear Energy*, Vol. 64, pp. 1-7 (2014).

[14] A. Abedi, N. Vasoughi, "Neutronic simulation of a pebble bed reactor considering its double heterogeneous nature", *Nuclear Engineering and Design,* Vol. 253, pp. 277-284 (2012).

[15] M. Goto, et al., "Impact of revised thermal neutron capture cross section of carbon stored in JENDL-4.0 on HTTR criticality calculation ", *Journal of Nuclear Science and Technology*, Vol. 48, No. 7, pp.965-969 (2011).

[16] J. Leppänen, M. DeHart, "HTGR reactor physics and burnup calculations using the Serpent Monte Carlo code", Trans. Am. Nuc. Soc., Vol. 101, pp. 782-784 (2009).

[17] J. Kim, G Kim, C. Huh, "Assessment of double heterogeneity treatment capability in SCALE", Proc. of the 22nd International Conference Nuclear Energy for New Europe, (2013).

[18] D. Ilas, J. Gehin, "HTTR fuel block simulations with SCALE", Proc. of PHYSOR 2010, Pittsburgh, U.S.A., (2010).

[19] J. Žáková, A. Talamo, "Criticality assessment for prismatic high temperature reactors by fuel stochastic Monte Carlo modeling", *Annals of Nuclear Energy*, Vol. 35, pp. 856-860 (2008).

[20] M.-H. Chiang, et al., "Evaluation of the HTTR criticality and burnup calculations with continuous-energy and multigroup cross sections", *Nuclear Engineering and Design*, Vol. 271, pp. 327-331 (2014).

[21] J. Leppänen, "Development of a new Monte Carlo reactor physics code", PhD Thesis, Helsinki University of Technology (2007).

[22] ORNL/TM-2005/39: "SCALE: A comprehensive modeling and simulation suite for nuclear safety analysis and design", Version 6.1, Oak Ridge National Laboratory, U.S.A., (2011).

[23] J. Leppänen, *private communication* (2014).

[24] R. J. Ellis, et al., "Generation of a broad-Group HTGR library for use with SCALE", NUREG/CR-7106, ORNL/TM-2011/298, U.S. NRC, Oak Ridge National Laboratory, (2012).

[25] M. Ouisloumen, R. Sanchez, "A model for neutron scattering off heavy isotopes that accounts for thermal agitation effects", *Nuclear Science and Engineering*, Vol. 107, pp. 189-200 (1991).

[26] M. L. Williams, "Resonance self-shielding methodologies in SCALE 6", *Nuclear Technology*, Vol. 174, pp. 149-168 (2011).

[27] J.-Y. Wang, et al., "HTTR criticality calculations with SCALE6: Studies of various geometric and unit-cell options in modeling", Proc. of PHYSOR 2012, Knoxville, U.S.A., (2012).

[28] "Temperature effect on reactivity in VHTRC-1 core", VHTRC-GCR-EXP-001, CRIT-COEF, NEA/NSC/DOC(2008).

[29] R.W. Swanson, L.J. Harrison, "The effect of carbon crystal structure on treat reactor physics calculations", CONF-880911-23, DE89 003625, International Reactor Physics Conference, Jackson Hole, U.S.A. (1988).

[30] A.I. Hawari, V.H. Gillete, "Inelastic thermal neutron scattering cross sections for reactor-grade graphite", *Nuclear Data Sheets*, Vol. 118, pp. 176-178 (2014)

[31] M. Williams et al., "Development of a Statistical Sampling Method for Uncertainty Analysis with SCALE", Proc. of PHYSOR 2012, Knoxville, Tennessee, U.S.A., (2012).

[32] L. Mercatali, et al., "SCALE Modeling of Selected Neutronics Test Problems within the OECD UAM LWR's Benchmark", *Science and*

Technology of Nuclear Installations, Vol. 2013,
Article ID 573697 (2013).